Provided for non-commercial research and education use.
Not for reproduction, distribution or commercial use.

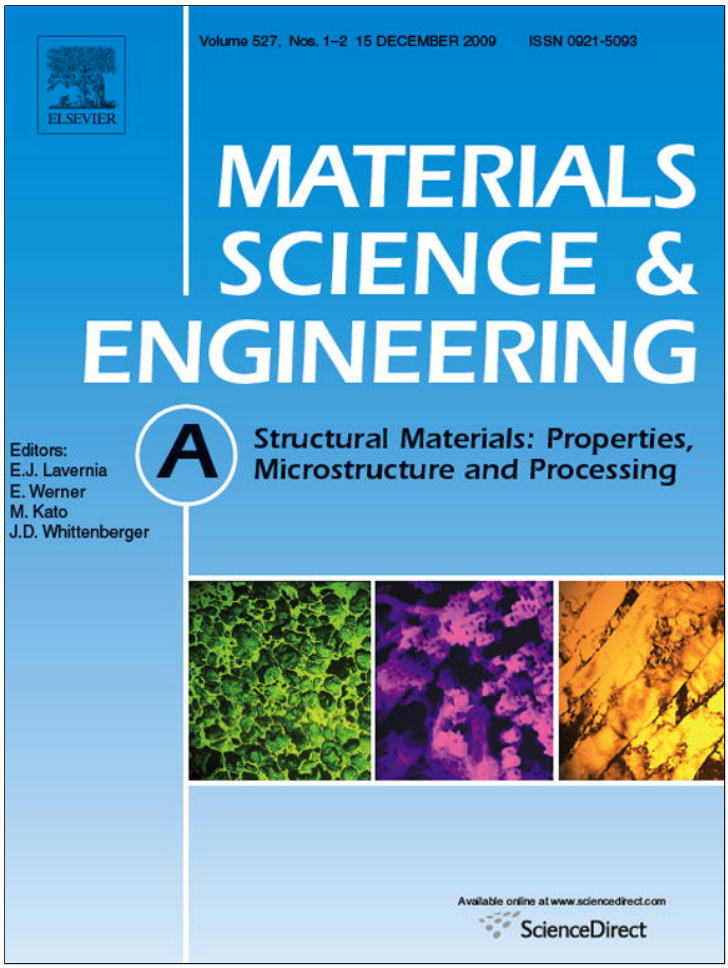

This article appeared in a journal published by Elsevier. The attached copy is furnished to the author for internal non-commercial research and education use, including for instruction at the authors institution and sharing with colleagues.

Other uses, including reproduction and distribution, or selling or licensing copies, or posting to personal, institutional or third party websites are prohibited.

In most cases authors are permitted to post their version of the article (e.g. in Word or Tex form) to their personal website or institutional repository. Authors requiring further information regarding Elsevier's archiving and manuscript policies are encouraged to visit:

http://www.elsevier.com/copyright

Author's personal copy

Materials Science and Engineering A 527 (2009) 61–64

Contents lists available at ScienceDirect

Materials Science and Engineering A

journal homepage: www.elsevier.com/locate/msea

Texture development of $Ca_3Co_4O_9$ thermoelectric oxide by high temperature plastic deformation and its contribution to the improvement in electric conductivity

H. Fukutomi*, Y. Konno, K. Okayasu, M. Hasegawa, H. Nakatsugawa

Department of Materials Science and Engineering, Graduate School of Engineering, Yokohama National University, 79-5 Tokiwadai, Hodogaya-ku, Yokohama, 240-8501, Japan

ARTICLE INFO

Article history:
Received 6 May 2009
Received in revised form 16 July 2009
Accepted 8 August 2009

Keywords:
Ca349
Thermoelectric oxide
Layered cobaltite
High temperature deformation
(0 0 1) Texture
Electric resistivity

ABSTRACT

High temperature uniaxial compression is conducted on $Ca_3Co_4O_9$ layered cobaltite, in order to achieve a thermoelectric oxide with low resistivity by the development of (0 0 1) texture. It is found that flow stress varies depending on deformation temperature and strain rate. Development of a sharp texture having the maximum (0 0 1) pole density of about 33 times as high as the random level is achieved. It is found that the high temperature compression process is quite effective for the simultaneous achievement of densification and (0 0 1) texture development. It is experimentally confirmed that resistivity decreases drastically by the construction of a sharp (0 0 1) texture.

© 2009 Elsevier B.V. All rights reserved.

1. Introduction

Cobalt oxides with layered structure (hereafter described as layered cobaltites) have been extensively explored as new thermoelectric materials for high temperature since the discovery of $NaCo_2O_4$ [1] as a promising oxide having low resistivity and high Seebeck coefficient. Recently, Masset et al. [2] reported $Ca_3Co_4O_9$ as a new high performance thermoelectric material of this kind of oxide. As the low resistivity originates from the high in-plane electrical conductivity on (0 0 1) of CoO_2 layer, process developments to achieve the textured state of polycrystalline layered cobaltites have been challenged by many researchers. Various methods such as reactive templated grain growth [3], hot pressing [4], magnetic texturation [5], sinter-forging [6] and thermoforging [7] have been proposed; most of them are designed on the basis of the rotation of oxide powder platelets by the application of pressure before and/or during the sintering.

One of the authors has developed a method for the simultaneous achievement of texture evolution and densification of the sintered bulk oxide by the high temperature compression deformation. In the method, the condition for the compression deformation is carefully selected in order to activate not only slip systems but also diffusion assisted phenomena such as diffusion creep, grain boundary sliding and dynamic recrystallization, necessary for maintaining the deformation continuity among crystal grains consisting the polycrystalline oxides. The process was already applied to $Bi_{1.5}Pb_{0.5}Sr_{1.7}Y_{0.5}Co_2O_{9-\delta}$ with layered structure; the composition was chosen to increase the concentration of structural vacancies [8]. It was found that the oxide could be heavily deformed without fracture and a sharp (0 0 1) texture was constructed. Drastic reduction in the resistivity was experimentally confirmed. In this study, the method found in the previous work was applied to $Ca_3Co_4O_9$ having the layered structure different from $Bi_{1.5}Pb_{0.5}Sr_{1.7}Y_{0.5}Co_2O_{9-\delta}$. In the case of $Bi_{1.5}Pb_{0.5}Sr_{1.7}Y_{0.5}Co_2O_{9-\delta}$, dielectric region consists of four layers, while three layers of CaO and CoO built the dielectric region in $Ca_3Co_4O_9$ as will be shown in Fig. 1. It was found that the method is valid for the development of (0 0 1) texture and the remarkable reduction in resistivity of $Ca_3Co_4O_9$, which seems to be close to the practical level.

2. Experimental procedure

$Ca_3Co_4O_9$ powders are synthesized by the citrate method in Seimi Chemical Co., Ltd. The powders are in a platelet form with the average size of 6.3 μm $\phi \times$ 1.5 μm. The powders were pressed into pellets at room temperature (cold press) under 200 MPa, followed by the final sintering in air at 1193 K for 24 h. The size of

* Corresponding author. Tel.: +81 45 339 3869; fax: +81 45 339 3869.
E-mail address: fukutomi@ynu.ac.jp (H. Fukutomi).

0921-5093/$ – see front matter © 2009 Elsevier B.V. All rights reserved.
doi:10.1016/j.msea.2009.08.012

Author's personal copy

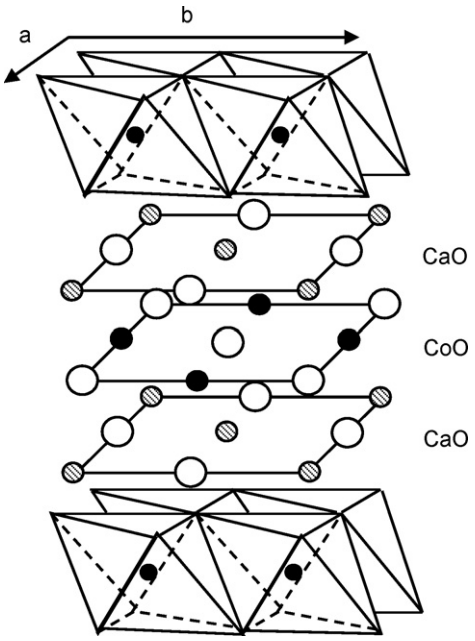

Fig. 1. Crystal structure of $Ca_3Co_4O_9$.

the specimen after cold pressing is 14 mm $\phi \times$ 13 mm. Compression deformation is conducted by an Instron type testing machine using MgO plates with strain rates of $1.3 \times 10^{-5}\,s^{-1}$ and $1.3 \times 10^{-4}\,s^{-1}$ and temperatures of 1153 K and 1193 K up to a true strain of −1.5. As for high temperature deformation, it is well known that deformation becomes easier with increasing temperature. However, it was reported that $Ca_3Co_4O_9$ decomposes at about 1223 K [9]. Hence differential thermal analysis was conducted to determine the temperature for the target phase structure; 1153 K and 1193 K are thus selected for the deformation temperature.

After the compression, mid-plane section was taken out by polishing for the texture measurements. Texture is measured by the Schulz reflection method using nickel filtered Cu Kα radiation. The texture is evaluated by (0 0 1) pole figure constructed on the basis of X-ray intensity of 0 0 1 0 reflection. Electric resistivity is measured by the usual four-probe method in the temperature range from 573 K to 1073 K in air.

3. Basis for the texture control

It is known that textures appear after deformation and recrystallization of metals and alloys. The essential part of texture development, namely the generation of uneven distribution of crystal orientations in polycrystals, is considered to be deformation, because no texture appears after the recrystallization of materials without textures in the deformed state. In the case of metals and alloys, textured state can be easily produced by cold working because of the excellent workability. In the case of ceramics, including oxide, texture development by cold working has never been achieved because of their brittleness. Therefore, how to plastically deform the polycrystalline is the basic issue to obtain the textured state in oxides.

As mentioned in the introduction, preferential alignment of (0 0 1) is important for the layered cobaltites. It is known that slip deformation rotates the compression plane to the position parallel to the slip plane; this means that the (0 0 1) texture can be achieved if the slip deformation occurs preferentially on (0 0 1).

Fig. 1 shows the crystal structure of the present oxide. The crystal structure consists of two parts. One is the electrically conductive layer CoO_2, appearing as blocks in the top and bottom of the figure

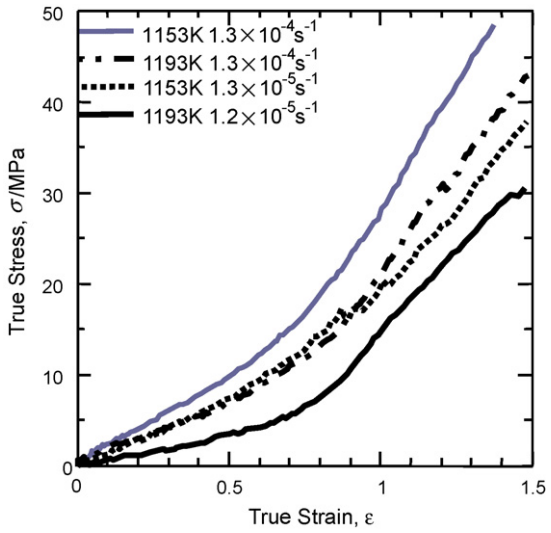

Fig. 2. Stress–strain curves at 1153 K and 1193 K.

and the other is the dielectric layers consisting of CaO and CoO. It is seen that the same atoms neighbor in ⟨1 1 0⟩ direction. Namely, the magnitude of Burgers vector is small in this direction of $Ca_3Co_4O_9$ in comparison with usual oxides having long periodic structure. It is expected that Peierls potential for the dislocations moving on (0 0 1) with Burgers vector of ⟨1 1 0⟩ direction may not be large. Thus, the deformation by the motion of this kind of dislocation might become possible with the help of thermal energy when the deformation is conducted at high temperatures.

Present method is basically planned on the basis of this consideration. High temperature has another meaning for the plastic deformation of this oxide. Fig. 1 shows that there are only two independent slip systems in (0 0 1)⟨1 1 0⟩, namely, von Mises criterion for deformation continuity in polycrystalline materials cannot be satisfied only by (0 0 1)⟨1 1 0⟩ dislocations. However, various kinds of deformation mechanism work at high temperatures; grain boundary sliding, dynamic recrystallization, etc. In order to supplement the lack of the numbers of independent slip systems described above, these kinds of additional deformation mechanisms should be activated. Hence the deformation is conducted under low strain rates such as $10^{-5}\,s^{-1}$ in this method in order to use diffusion assisted deformation mechanisms.

4. Results and discussion

4.1. Deformation behavior

Fig. 2 shows the stress–strain curves at two temperatures. Here absolute values of true strain are used. It is seen that flow stress monotonously increases with an increase in strain in all the deformation conditions. Namely work hardening appears. The increase in temperature as well as a decrease in strain rate results in the decrease in stresses. That is, flow stress depends on strain rate and temperature, which is the same tendency for the deformation of metals and alloys at high temperatures. As shown in Fig. 2, flow stress increases with an increase in strain up to −1.5. However, the slope of the curve, i.e. apparent work hardening rate, markedly increases around −0.9 to −1.0 in true strain. This suggests that the densification almost completes around these strains.

4.2. Densification process

Fig. 3 shows the density change with an increase in strain. The measurements were conducted on the middle part of the specimen.

Author's personal copy

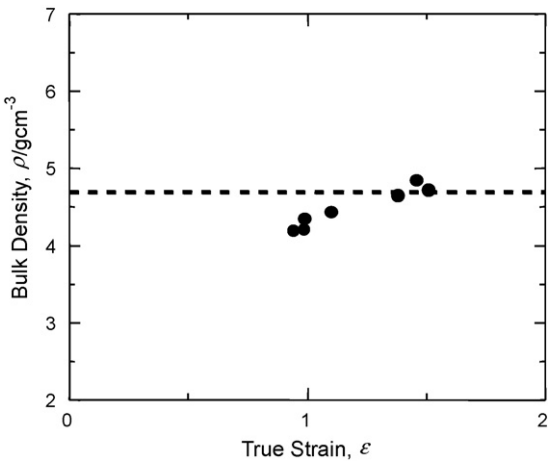

Fig. 3. Effect of high temperature deformation on the density.

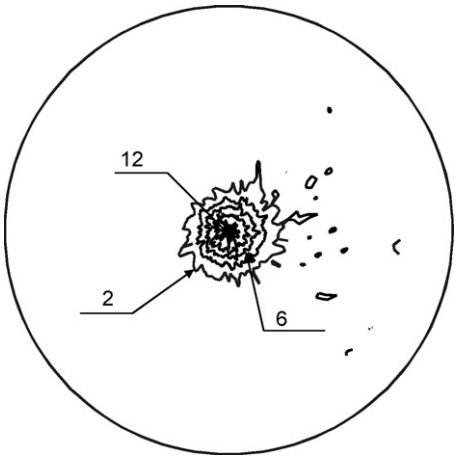

Fig. 5. (0 0 1) pole figure after the deformation at 1193 K with a strain rate of $1.3 \times 10^{-4}\,s^{-1}$ up to a true strain of −1.5.

Broken line shows the reported value of bulk $Ca_3Co_4O_9$ [10]. It is seen that the density becomes constant at about −1.2 in true strain. In the case of $Pb_{0.5}Sr_{1.7}Y_{0.5}Co_2O_{9-\delta}$ reported in the previous paper [8], the densification monotonously proceeds and completes at a true strain of about −0.9. This difference can be attributed to the difference in sintering temperatures. Sintering was conducted at 1113 K for $Pb_{0.5}Sr_{1.7}Y_{0.5}Co_2O_{9-\delta}$ which is about 94% of its melting point, while in the case of the present material, the sintering was conducted at 1193 K which is below 80% of its melting temperature.

4.3. Texture

Fig. 4 is a (0 0 1) pole figure showing a result of texture measurement after the deformation at 1193 K with a strain rate of $1.3 \times 10^{-5}\,s^{-1}$ up to a true strain of −1.5. Pole density is projected onto the compression plane. Mean pole density is used as a unit. It is seen that the pole densities are distributed in a concentric circular manner. This indicates a formation of fiber texture. The pole density is highest at the center of the pole figure; the main component of the texture is (0 0 1)(compression plane) which is expected on the basis of the examination on crystal structure. The level of the pole density at the center is 22 times of the mean pole density; it is experimentally confirmed that a sharp (0 0 1) texture is constructed by the present method.

Fig. 5 shows the (0 0 1) pole figure after the deformation at 1193 K with a strain rate of $1.3 \times 10^{-4}\,s^{-1}$ up to a true strain of −1.5. Comparison of Fig. 4 with Fig. 5 indicates that the basic feature of pole density distribution is the same for these two cases. The difference is the sharpness of the texture. While the maximum pole density I_{max} in Fig. 4 is 22, that of Fig. 5 is 12. Namely, the texture sharpness varies depending on the deformation conditions. In the present study, maximum value of I_{max} is 33 where deformation was conducted at 1153 K with a strain rate of $1.3 \times 10^{-5}\,s^{-1}$.

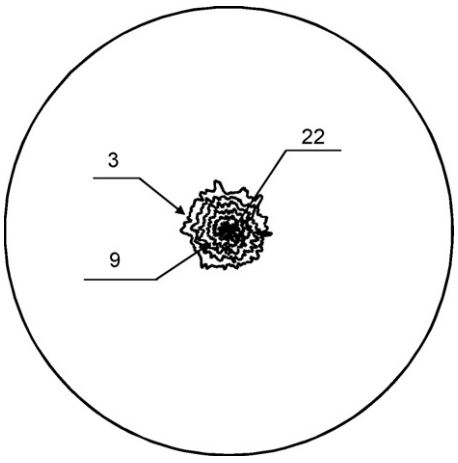

Fig. 4. (0 0 1) pole figure after the deformation at 1193 K with a strain rate of $1.3 \times 10^{-5}\,s^{-1}$ up to a true strain of −1.5.

Fig. 6(a) and (b) show the microstructure observed at the cross section after the deformation by scanning electron microscope. Fig. 6(a) and (b) correspond to the textures given in Figs. 4 and 5, respectively. The specimens are produced by the thermal etching at 1193 K for 16 h after polishing. It is seen that the microstructure of the specimen produced by the strain rate of $1.3 \times 10^{-5}\,s^{-1}$ consists of large grains which seem to be slightly elongated towards the side direction while that of the specimen produced by a strain rate of $1.3 \times 10^{-4}\,s^{-1}$ consists of the mixture of large and fine grains. The aspect ratio (grain length perpendicular to the compression direction/grain length along compression direction) of the grains in Fig. 6(a) is about 1.4. This clearly suggests that the crystal grains are plastically deformed. The aspect ratio, however seems to be smaller than that expected from the amount of compression strain.

Crystal structure shown in Fig. 1 indicates that two independent slip systems having (0 0 1) slip plane might be activated at high temperatures. This promotes the rotation of (0 0 1) to the position parallel to the compression plane. However, slip deformation with a strain component along *c*-axis by the motion of dislocations is not expected due to the long periodicity of the crystal structure. Therefore, once the (0 0 1) becomes almost parallel to the compression plane by the slip on (0 0 1), no further increase in aspect ratio is expected. As shown in Fig. 6(a) and (b), no obvious cracks are seen after deformation. This means that compliment mechanisms other than slip deformation works at high temperatures, otherwise polycrystalline material cannot deform plastically. In the case of Fig. 6(a), crystal grains are larger than that before deformation. This suggests that diffusion might contribute to the plastic deformation. On the other hand, Fig. 6(b) suggests two possibilities. One is the occurrence of dynamic recrystallization and the other is the smash of $Ca_3Co_4O_9$ powders during deformation. As shown in Fig. 2, all the stress–strain curves show work hardening and no distinct softening is seen, occurrence of dynamic recrystallization is not considered. It can be said that plastic deformation is suppressed in Fig. 6(b) in comparison to Fig. 6(a), which results in the formation of texture weaker than that for the deformation corresponding to Fig. 6(a).

Author's personal copy

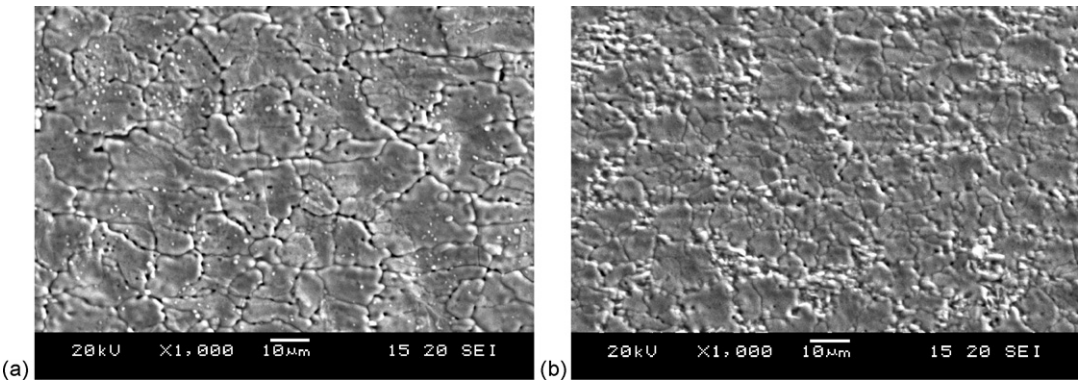

Fig. 6. (a and b) Microstructure observed at cross section of the specimen after the deformation at 1193 K up to a strain of −1.5, with strain rates of (a) $1.3 \times 10^{-5}\ s^{-1}$ and (b) $1.3 \times 10^{-4}\ s^{-1}$.

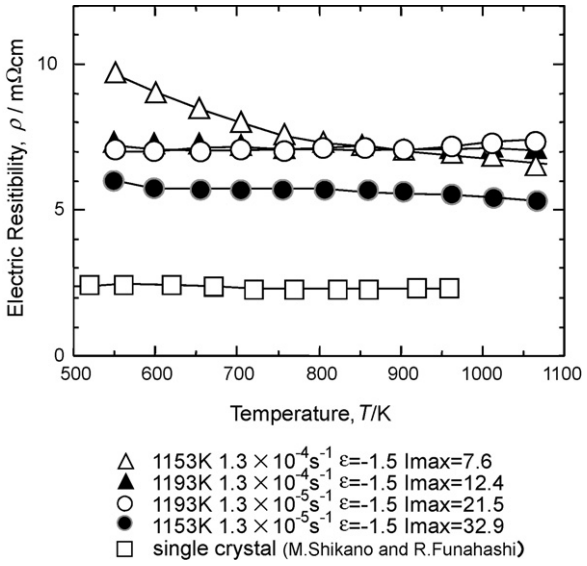

Fig. 7. Effect of texture development on resistivity measured at 573–1073 K. I_{max} is the maximum pole density for (0 0 1).

4.4. Resistivity

Fig. 7 shows the results of resistivity measurements conducted in the temperature range from 573 K to 1073 K. The measurement was conducted in the direction parallel to the specimen surface; namely in-plane resistivity is measured. Resistivity is measured both by heating and cooling runs. No big differences are seen in the values measured during heating and cooling. The measured value of resistivity is about 10 mΩ cm at 573 K and decreases with an increase in temperature until 5.4 mΩ cm at 1073 K. According to the literature, resistivity in the as sintered state without texture is about 30 mΩ cm at 400 K [7]. The present value 5.4 mΩ cm is about twice of the reported value on a single crystal at the same temperature. It is thus concluded that the method shown in this paper is quite effective to improve the electric conductivity based on texture control. It should be emphasized that the present process needs no special equipments and hence has a high applicability to various ceramics.

5. Conclusions

In order to produce the (0 0 1)(compression plane) textured polycrystalline $Ca_3Co_4O_9$ oxide, high temperature deformation was conducted in the uniaxial mode. Major results are summarized as follows.

(1) $Ca_3Co_4O_9$ cobaltite can be heavily deformed at high temperatures. The deformation up to a true strain of −1.5 is possible at 1153 K and 1193 K.
(2) The flow stress at high temperature deformation varies depending on strain rate and deformation temperature. This suggests that the deformation can be attributed to the plastic deformation and not the relative translation of the powders in the platelet shape.
(3) (0 0 1) (compression plane) texture develops by the compression deformation. The maximum pole density is about 33 times as high as the random level.
(4) The electric resistivity drastically decreases with the development of (0 0 1) texture. The lowest value is about twice as high as the reported value of a single crystal, which is close to the level for practical application.

Acknowledgement

The authors thank Mr. S. Takayasu for his help in the experiments. The financial support of JSPS is greatly appreciated.

References

[1] I. Terasaki, Y. Sasago, K. Uchinokura, Phys. Rev. B 56 (1997) R12685–R12687.
[2] A.C. Masset, C. Michel, A. Maignan, M. Hervieu, O. Toulemonde, F. Studer, B. Raveau, Phys. Rev. B62 (2000) 166–175.
[3] T. Tani, H. Itahata, C. Xia, J. Sugiyama, J. Matar. Chem. 13 (2003) 1865–1867.
[4] E. Guilmeau, R. Funahashi, M. Mikami, K. Chong, D. Chateigner, Appl. Phys. Lett. 85 (2004) 1490–1492.
[5] Y. Zhou, I. Matsubara, S. Horii, T. Takeuchi, R. Funahashi, M. Shikano, J. Shimoyama, K. Kishio, W. Shin, N. Izu, N. Murayama, J. Appl. Phys. 93 (2003) 2653–2658.
[6] W. Shin, N. Murayama, J. Mater. Res. 15 (2000) 382–386.
[7] M. Prevel, S. Lemonnier, Y. Klein, S. Hébert, D. Chateigner, B. Ouladdiaf, J.G. Noudem, J. Appl. Phys. 98 (2005) 093706–093711.
[8] H. Fukutomi, E. Iguchi, N. Ogawa, Mater. Sci. Forum 495–497 (2005) 1407–1412.
[9] M. Sopicka-Lizer, P. Smaczyński, K. Kozłowska, E. Bobrowska-Grzesik, J. Plewa, H. Altenburg, J. Eur. Ceram. Soc. 25 (2005) 1997–2001.
[10] R. Funahashi, I. Matsubara, H. Ikuta, T. Takeuchi, U. Mizutani, S. Sodeoka, Jpn. J. Appl. Phys. 39 (2000) L1127–L1129.